PROCEEDINGS OF SCIENCE

The Acoustic Calibration System for the Pacific Ocean Neutrino Experiment

Dilraj Ghuman,[a,*] **Felix Henningsen**[a] **and Matthias Danninger**[a] **for the P–ONE Collaboration**

[a] *Simon Fraser University, Physics*
8888 University Dr W, Burnaby, Canada
E-mail: dilraj_ghuman@sfu.ca, felix_henningsen@sfu.ca, matthias.danninger@cern.ch

The Pacific Ocean Neutrino Experiment (P-ONE) is a proposed neutrino telescope that will explore the deepest reaches of the universe through cosmic neutrinos. Located 2600 meters below sea-level in the Cascadia Basin off the coast of Vancouver, Canada, the detector will utilise Cherenkov radiation from secondary particles emitted by high energy neutrino interactions as a means of detection. These emissions are digitized by optical modules lining the vertically deployed strings. Accordingly, the accuracy of detection will directly correlate with the understanding of the medium, and the locations of the optical modules. The ocean currents present a hurdle in this respect. A common tracking method is utilising acoustic detectors and emitters in a methodology known as trilateration. The acoustic modules will use piezoelectric disks to detect the vibrations produced by acoustic beacons for this calibration process. P-ONE will be designed with these additional acoustic detectors for tracking, and will be tested with Ocean Networks Canada's Marine Test Facility. In this contribution we will cover the simulated performance of the acoustic trilateration and the status of the P-ONE Acoustic Calibration System.

38th International Cosmic Ray Conference (ICRC2023)
26 July - 3 August, 2023
Nagoya, Japan

ICRC2023
38th International Cosmic Ray Conference
The Astroparticle Physics Conference

*Speaker

PoS(ICRC2023)1112

1. Pacific Ocean Neutrino Experiment

The Pacific Ocean Neutrino Experiment (P–ONE) is the proposed cubic-kilometer neutrino telescope that will be located in the Cascadia Basin off the West coast of Canada [3]. P–ONE will probe the deepest reaches of the Universe [3] by utilizing the Cerenkov emissions [6] of secondaries produced by neutrino interactions in the aquatic volume. The neutral nature of the neutrino makes it an ideal candidate for probing astroparticle physics of the most energetic objects in and outside the galaxy. The key to a successful neutrino telescope endeavour is optimizing for coverage of the sky and detector volume. The P–ONE detector will significantly increase sky coverage of the global neutrino astronomy effort, adding to the existing IceCube detector [1] and the KM3NeT detectors [2] in the Mediterranean. This will further the mutual goals of all neutrino telescopes and push towards a better understanding of the cosmos we are surrounded by.

The clustered design is optimized for a large–volume detector that maintains granularity for accurate pointing reconstructions. The reconstruction of the full P–ONE detector will be tested and verified with the installation of the P–ONE demonstrator [7]. There are however systematics that can impact the reconstruction. One such systematic is the medium itself. By choosing to deploy in the ocean, the benefit of a large–volume array comes at the cost of a wild environment. The currents of the water will result in the detector swaying in time due to the design of the detector being cabled mooring lines attached to buoys. If untracked, the motion will lead to errors in the location of the modules and thus limit the accuracy of the reconstruction. For this reason, the detector will have to undergo constant calibration with the purpose of tracking the movement of the strings down to the individual module level. There are two potential means of calibration; the novel approach by P–ONE will be to use optical calibrators [9] alongside the acoustic.

2. Acoustic Multilateration

Calibrating the motion of modules underwater to centimetre precision is inherently a non-trivial task. The standard means of tracking motion underwater is through acoustics, and hence will be one of the ways that the P–ONE detector will track modules. This method is similar to that of GPS, where time-of-arrival data is used to reconstruct the locations of objects. The method here is referred to as *Acoustic Multilateration*.

The basics of trilateration are to use the difference in time-of-arrival between distinct sources to determine the location of the module. As we can see in figure 1, the causal position of the module can be reconstructed using the three beacons at known positions and the speed of sound in the medium. This idea naturally extends to three dimensions, where here we have shown two for simplicity. It is preferential to over constrain the system with more beacons than necessary for a position calibration as

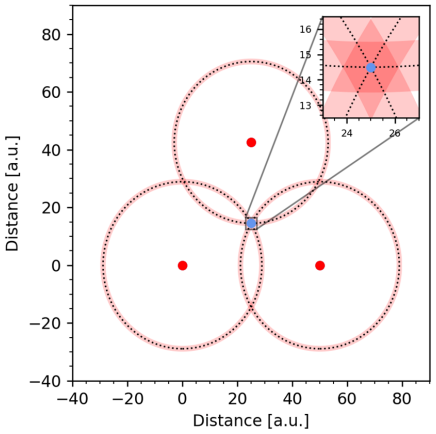

Figure 1: Simple illustration of three beacons surrounding a single module. The wavefronts are showcased with some width to represent error in timing.

the extra information can help reduce systematic uncertainties. On the other hand, under constraining the system leads to sets of solutions with degeneracy and hence large uncertainty in the final solution.

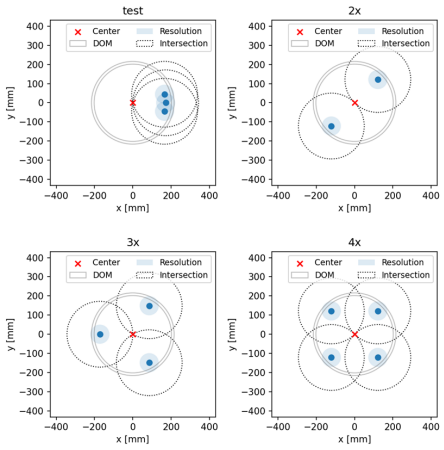

Figure 2: Four potential geometric locations of receivers are shown in the images above. The 'test' figure is primarily to show the effect of a 'single' receiver.

A Markov pseudo-experiment is run with some Gaussian distributions as errors on the known parameters as a means of understanding the posterior distribution of results. The result is then a minimization of a χ^2 distribution. This can be repeated for a brute force computation of the result distribution also known as the posterior. Four geometries were tested and compared in figure 2. There are two key findings that arise from this study. As expected, the number of beacons determines the accuracy with which we can distinguish the location of the module. Moreover, with the 'test' and '2x' geometries, there are degeneracies that aren't resolved and lead to an infinite set of solutions.

The second finding is that the uncertainty of the beacon heavily impacts the accuracy of the predicted module location. Figure 3 shows two sets of data with different applied uncertainties to the emitter/beacon locations. In comparing the results of figure 3a and figure 3b we see that the largest impact will be from the uncertainty in the locations of the beacons.

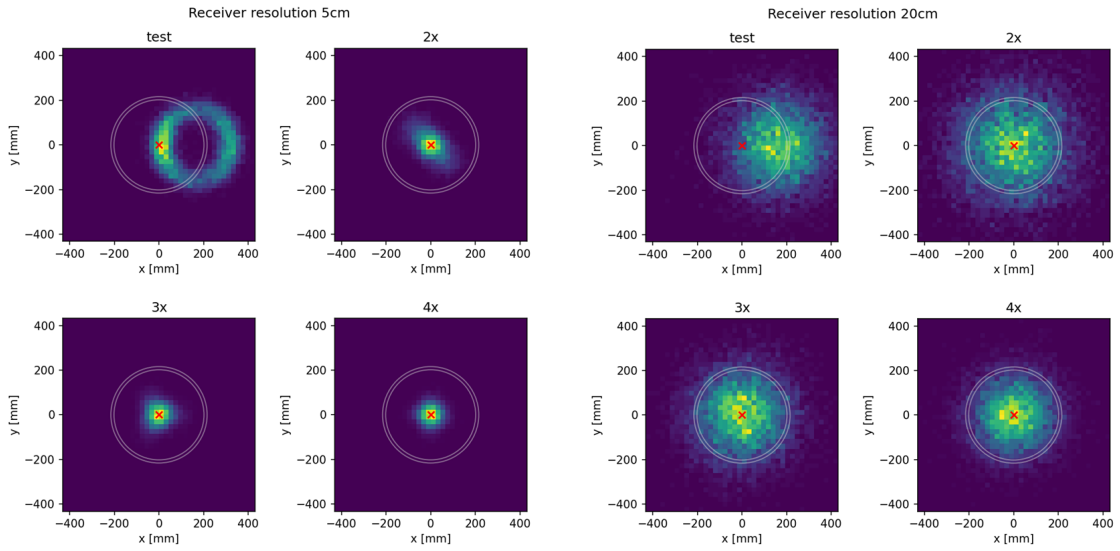

(a) **(b)**

Figure 3: The four different geometries are compared in their effectiveness of resolving the module centre. In **(a)**, the beacons are assumed a 5cm error in position, and in **(b)** the error is assumed to be 20cm. The error in the receiver location severely impacts the ability to resolve the centre of the module and hence would be the dominating error in the reconstruction.

This problem of accurately placing equipment underwater leads naturally to a collaboration with the Northern Cascadia Subduction Zone Observatory (NCSZO) [5]. The NCSZO, located in the Neptune Observatory of Ocean Networks Canada (ONC), will track the shifting tectonic plates to monitor megathrust earthquakes from the Cascadia fault line [5]. These shifts of the tectonic plates are monitored by using beacons anchored to the seafloor whose locations are tracked using a 'waveglider' [4, 5]. In figure 4 we see from subfigure **(c)** an example of how this waveglider technology works, but rather than a boat being used as an intermediary, there is a small glider that sits on the surface of the water for NCSZO. By collaborating with this observatory, the P–ONE acoustic calibration beacons can get calibrated in absolute location.

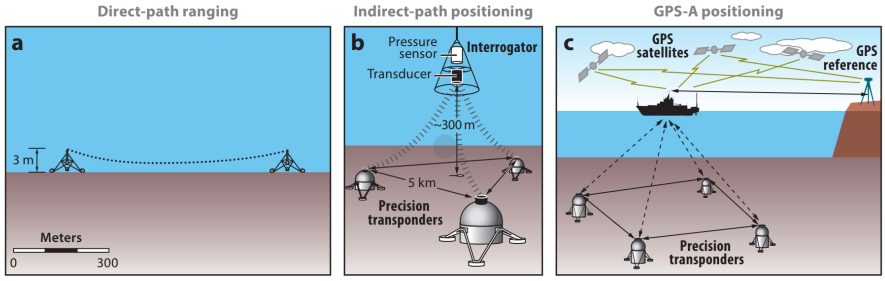

Figure 4: This graphic from [4] shows the three standard ways of monitoring the locations of beacons for the purposes of geodesy. In **a** we see the simple direct method that is used in the study above. In **b** we see the the use of an intermediate interrogator that has a known location for calibration. In **c** we see the most accurate method of using a GPS tracked ship (or in the case of NCSZO, a waveglider) which can then probe the beacons.

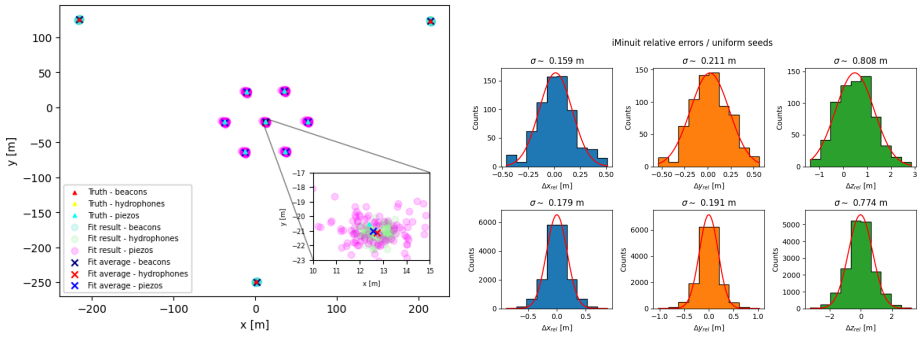

(a) **(b)**

Figure 5: In **(a)** we see what 100 reconstructions of normal priors on the truths look like. There is a clear clustering around the truth in this 2D projection, and shows the capibilities of the beacons to calibrate other beacon positions aswell. In **(b)** we see the errors in these reconstructions histogramed with the intra-(top) and inter-string(bottom) hydrophone and piezoelectric receivers extracted from different truth value fits.

3. Acoustic Receiver

The previous toy models describe the process by which the acoustic tracking would be done. The hardware is currently being designed and tested for the first (and future) deployment of the

P-ONE neutrino telescope. To achieve the goal of tracking the locations of the modules, each optical module will have to be fitted with acoustic receivers. These will be capable of converting the acoustic signal output from the acoustic beacons on the seafloor into usable data for the final tracking software. For this purpose the choice of transducer is a piezoelectric disk that can convert the acoustic energy into electrical signals. The signal will be amplified and passed to a mainboard with an analog-to-digital converter (ADC). The piezoelectric disk and amplifier will be housed in an aluminum shield which will act as electromagnetic shielding.

3.1 Amplification

Amplification of the piezoelectric signal is needed to increase sensitivity to acoustic signals transmitted over long distances in water and through the glass pressure housing. An amplifier for the P-ONE acoustic receivers was designed based on the IceCube Upgrade acoustic system [8]. Figure 6a and 6b show the prototype schematic and pre-amplifier board respectively.

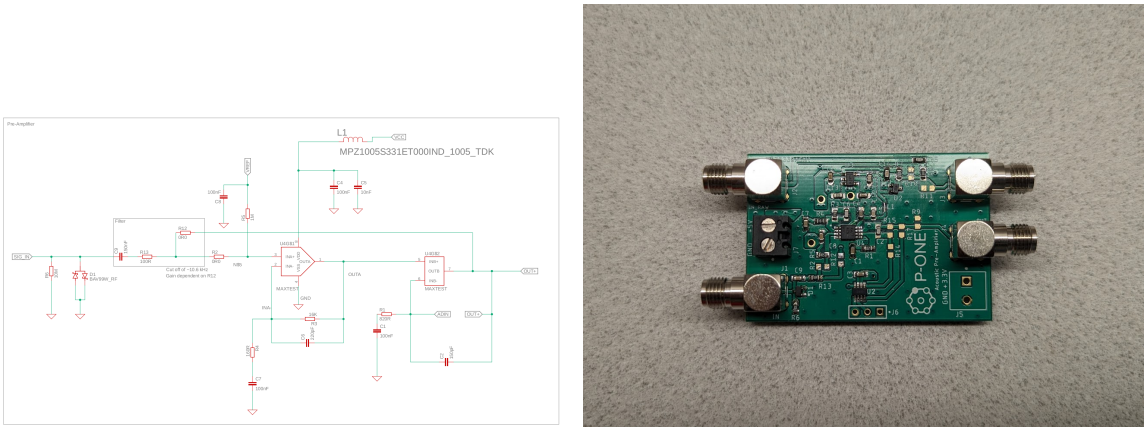

(a) **(b)**

Figure 6: The schematic for a test pre-amplifier (left) provides some flexibility for testing and replacing parts. By having a spacious layout on the board (right) we see that there is plenty of room to add or short certain parts as needed.

The key component of the amplification process is the MAX4477AUAT amplifier. The acoustic signals picked up by the piezoelectric are amplified here, and eventually fed to an ADC – or an oscilloscope – for further analysis. The board has a digital potentiometer which allows for variable resistance control via Serial Peripheral Interface (SPI). This allows for SPI controlled dynamic gain of the amplification chain.

3.2 Test Setup

The goal of this setup is to minimize external acoustic noise during prototyping and testing. This is achieved with a 'quiet' box padded with two layers of acoustic foam, seen in figure 7. Inside the box is a receiver that is being tested, and an emitter fed by a trigger generator for acoustic pulses. These are both attached to a Rohde & Schwarz RTM3004 oscilloscope. The oscilloscope produces the signal that is passed to the emitter and hence has a trigger based off of the output signal to synchronize with the receiver. With this setup, the response of the receiver to varying amplitude

and frequency of waveforms can be tested. The detected waveform is then Fourier-transformed for frequency analysis, as seen in figure 8. The measured voltage ratio between receiver and emitter gives an idea of its performance at various frequencies. The results for this test with a prototype piezoelectric disk are observed in figure 9a.

We see that there is a clear peak in response at around 150 kHz. This is expected to be from the resonance frequency of the piezoelectrics. The large difference between the amplified and the un-amplified responses are the scale of the response. The gain of the amplifier was fixed to 1000 for the sake of these tests, and this three order of magnitude scaling is evident in the plots. The benefit of the amplifier is exactly this, as the signal will be easier to see above the noise. This does mean that noise is also amplified, and hence there is some optimal gain where the signal of interest is optimally amplified.

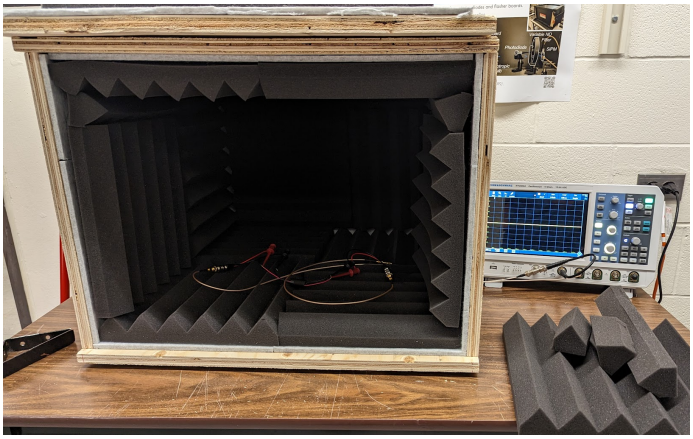

Figure 7: The box is made of plywood and lined with two layers of acoustic foam for reducing noise. This only has meaningful impact on audible frequencies, but will reduce any external noise in the lab or around the area.

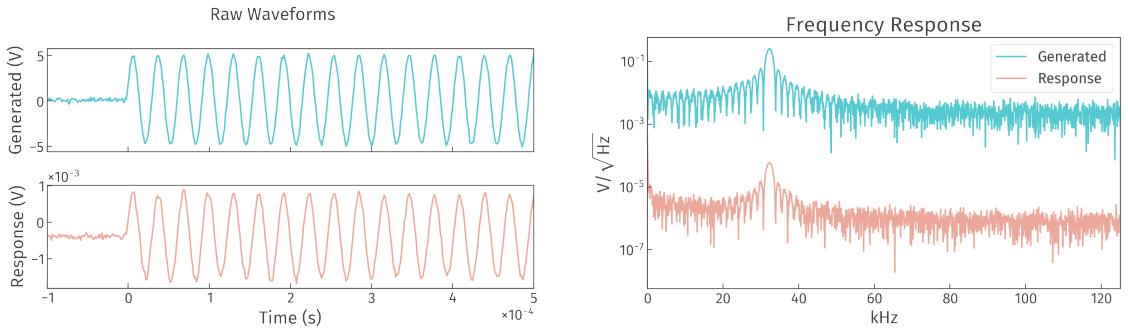

(a) **(b)**

Figure 8: We see the raw waveforms (left) for a signal sent by the oscilloscope and then the response from the piezoelectric as it receives it. Taking the Fourier transform of these results gives the frequency breakdown of the generated waveform and the response waveform (right).

3.3 Housing Design

For the purpose of protecting the piezoelectric and the amplifier from electromagnetic radiation and keeping it all in place, there needs to be a housing. The current model of includes an inner capsule made of plastic that will interface the PCB pre-amplifier with the piezoelectric while keeping them both in place. This plastic piece will then fit into an aluminum exterior that will act as

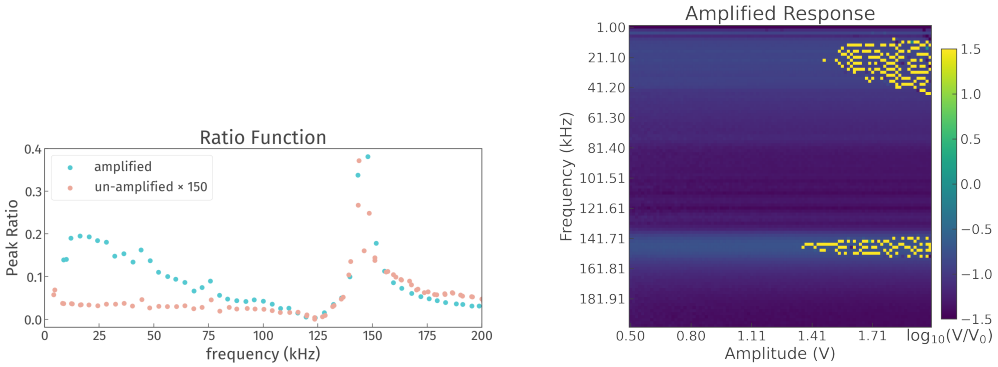

(a) **(b)**

Figure 9: In **(a)** we have the comparison of the response ratio from the amplified and un-amplified. For comparison the un-amplified is scaled up by a factor of 150 so they both show up on the same scale. Clearly both plots feature the same piezoelectric resonance peak at approximitaly 150 kHz. The amplified ratio also has a linear fall-off with frequency as the amplifier performs better for lower frequencies. In **(b)** we see a full sweep of the frequency-amplitude space for the generated pulse. The z-axis is the logarithm of the ratio due to the large swings in the response. There are artefacts that we believe are due to oscilloscope limitations that we are currently addressing.

electromagnetic shielding. Epoxy will be used to interface the piezoelectric disk and plastic inner capsule with the glass. This will keep the acoustic receiver from shifting and moving around.

(a) **(b)**

Figure 10: Solidworks images of the assembled (left) and exploded (right) housing of the acoustic receiver. The threading will allow for the capsule to be screwed into the exterior and apply pressure to the PCB keeping it in place. No PCB has been fit into the assembly in this drawing, but there is a cavity where it will be inserted. The gold part is the piezoelectric disk with a 20 cm diameter.

4. Next Steps

With a prototype under construction, our next steps will be to test the acoustic receiver in a submerged environment. The acoustic receiver will be mounted inside a test hemisphere rigged to on end of a submergable platform with the help of ONC. This system comprises of a calibrated acoustic beacon and hydrophone, in addition to the to-be-tested acoustic device. The performance of the understood beacon-receiver response will provide a baseline of performance improvements needed for the acoustic receiver.

Acknowledgments

We thank Ocean Networks Canada for the very successful operation of the NEPTUNE observatory, as well as the support staff from our institutions without whom P-ONE could not be operated efficiently.

We acknowledge the support of Natural Sciences and Engineering Research Council, Canada Foundation for Innovation, Digital Research Alliance, and the Canada First Research Excellence Fund through the Arthur B. McDonald Canadian Astroparticle Physics Research Institute, Canada; European Research Council (ERC), European Union; Deutsche Forschungsgemeinschaft (DFG), Germany; National Science Centre, Poland; U.S. National Science Foundation-Physics Division, USA.

References

[1] M.G. Aartsen, M. Ackermann, J. Adams, J.A. Aguilar, M. Ahlers, M. Ahrens, D. Altmann, K. Andeen, T. Anderson, I. Ansseau, and et al. The icecube neutrino observatory: instrumentation and online systems. *Journal of Instrumentation*, 12(03):P03012–P03012, Mar 2017.

[2] S Adrián-Martínez, M Ageron, F Aharonian, S Aiello, A Albert, F Ameli, E Anassontzis, M Andre, G Androulakis, M Anghinolfi, and et al. Letter of intent for km3net 2.0. *Journal of Physics G: Nuclear and Particle Physics*, 43(8):084001, Jun 2016.

[3] Matteo Agostini, Michael Böhmer, Jeff Bosma, Kenneth Clark, Matthias Danninger, Christian Fruck, Roman Gernhäuser, Andreas Gärtner, Darren Grant, Felix Henningsen, and et al. The pacific ocean neutrino experiment. *Nature Astronomy*, 4(10):913–915, Sep 2020.

[4] Roland Bürgmann and David Chadwell. Seafloor geodesy. *Annual Review of Earth and Planetary Sciences*, 42(1):509–534, 2014.

[5] Joseph J. Farrugia, Martin Heesemann, Martin Scherwath, Kate Moran, Earl Davis, Kelin Wang, Yan Jiang, Joe Henton, David Chadwell, Evan Solomon, Rachel Lauer, and Geraint R. West. Northern cascadia subduction zone observatory (ncszo): an interdisciplinary research initiative to assess tsunami and earthquake hazard from the cascadia megathrust. In *OCEANS 2019 MTS/IEEE SEATTLE*, pages 1–8, 2019.

[6] V. L. Ginzburg. Radiation from uniformly moving sources (vavilov-cherenkov effect, transition radiation, and some other phenomena). *Acoustical Physics*, 51, Feb 2005.

[7] Felix Henningsen. Pacific ocean neutrino experiment: Expected performance of the first cluster of strings. *PoS*, ICRC2023:1053, 2023.

[8] Moritz Kellermann. Entwicklung akustischer sensoren für ein kalibrierungssystem für die geometrie des icecube upgrades. Technical report, Rhine-Westphalia Technical University of Aachen, May 2020.

[9] Jakub Stacho. Development of calibration light sources for the pacific ocean neutrino experiment. *PoS*, ICRC2023:1113, 2023.

Full Authors List: P–ONE Collaboration

Matteo Agostini[11], Nicolai Bailly[1], A.J. Baron[1], Jeannette Bedard[1], Chiara Bellenghi[2], Michael Böhmer[2], Cassandra Bosma[1], Dirk Brussow[1], Ken Clark[3], Beatrice Crudele[11], Matthias Danninger[4], Fabio De Leo[1], Nathan Deis[1], Tyce DeYoung[6], Martin Dinkel[2], Jeanne Garriz[6], Andreas Gärtner[5], Roman Gernhäuser[2], Dilraj Ghuman[4], Vincent Gousy-Leblanc[2], Darren Grant[6], Christian Haack[14], Robert Halliday[6], Patrick Hatch[3], Felix Henningsen[4], Kilian Holzapfel[2], Reyna Jenkyns[1], Tobias Kerscher[2], Shane Kerschtien[1], Konrad Kopański[15], Claudio Kopper[14], Carsten B. Krauss[5], Ian Kulin[1], Naoko Kurahashi[12], Paul C. W. Lai[11], Tim Lavallee[1], Klaus Leismüller[2], Sally Leys[8], Ruohan Li[2], Paweł Malecki[15], Thomas McElroy[5], Adam Maunder[5], Jan Michel[9], Santiago Miro Trejo[5], Caleb Miller[4], Nathan Molberg[5], Roger Moore[5], Hans Niederhausen[6], Wojciech Noga[15], Laszlo Papp[2], Nahee Park[3], Meghan Paulson[1], Benoît Pirenne[1], Tom Qiu[1], Elisa Resconi[2], Niklas Retza[2], Sergio Rico Agreda[1], Steven Robertson[5], Albert Ruskey[1], Lisa Schumacher[14], Stephen Sclafani[12 α], Christian Spannfellner[2], Jakub Stacho[4], Ignacio Taboada[13], Andrii Terliuk[2], Matt Tradewell[1], Michael Traxler[10], Chun Fai Tung[13], Jean Pierre Twagirayezu[6], Braeden Veenstra[5], Seann Wagner[1], Christopher Weaver[6], Nathan Whitehorn[6], Kinwah Wu[11], Juan Pablo Yañez[5], Shiqi Yu[6], Yingsong Zheng[1]

[1]Ocean Networks Canada, University of Victoria, Victoria, British Columbia, Canada.
[2]Department of Physics, School of Natural Sciences, Technical University of Munich, Garching, Germany.
[3]Department of Physics, Engineering Physics and Astronomy, Queen's University, Kingston, Ontario, Canada.
[4]Department of Physics, Simon Fraser University, Burnaby, British Columbia, Canada.
[5]Department of Physics, University of Alberta, Edmonton, Alberta, Canada.
[6]Department of Physics and Astronomy, Michigan State University, East Lansing, MI, USA.
[8]Department of Biological Sciences, University of Alberta, Edmonton, Alberta, Canada.
[10]Gesellschaft für Schwerionenforschung, Darmstadt, Germany.
[11] Department of Physics and Astronomy and Mullard Space Science Laboratory, University College London, United Kingdom
[12] Department of Physics, Drexel University, 3141 Chestnut Street, Philadelphia, PA 19104, USA.
[13] School of Physics and Center for Relativistic Astrophysics, Georgia Institute of Technology, Atlanta, GA, USA.
[14] Erlangen Centre for Astroparticle Physics, Friedrich-Alexander-Universität Erlangen-Nürnberg, D-91058 Erlangen, Germany.
[15] H. Niewodniczański Institute of Nuclear Physics, Polish Academy of Sciences, Radzikowskiego 152, 31-342 Kraków, Poland.
$^{\alpha}$ now at Department of Physics, University of Maryland, College Park, MD 20742, USA.

PoS(ICRC2023)1112